On the origin of the neutral hydrogen supershells: the ionized progenitors and the limitations of the multiple supernovae hypothesis

Sergiy Silich

Instituto Nacional de Astrofísica Optica y Electrónica, AP 51, 72000 Puebla, México; silich@inaoep.mx

Federico Elias

Instituto de Astronomía. Universidad Nacional Autónoma de México. AP 70 - 264, 04510 México D.F.; felias@astroscu.unam.mx

and

José Franco

Instituto de Astronomía. Universidad Nacional Autónoma de México. AP 70 - 264, 04510 México D.F.; pepe@astroscu.unam.mx

ABSTRACT

Here we address the question whether the ionized shells associated with giant HII regions can be progenitors of the larger HI shell-like objects found in the Milky Way and other spiral and dwarf irregular galaxies. We use for our analysis a sample of 12 HII shells presented recently by Relaño et al. (2005, 2007). We calculate the evolutionary tracks that these shells would have if their expansion is driven by multiple supernovae explosions from the parental stellar clusters. We find, contrary to Relaño et al. (2007), that the evolutionary tracks of their sample HII shells are inconsistent with the observed parameters of the largest and most massive neutral hydrogen supershells. We conclude that HII shells found inside giant HII regions may represent the progenitors of small or intermediate HI shells, however they cannot evolve into the largest HI objects unless, aside from the multiple supernovae explosions, an additional energy source contributes to their expansion.

Subject headings: ISM: bubbles — (ISM:) HII regions — ISM: kinematics and dynamics

1. Introduction

The origin of numerous holes and shells detected in the distribution of neutral hydrogen in spiral and dwarf galaxies (Heiles, 1980; Brinks & Bajaja, 1986; Puche et al., 1992) is a long standing problem (Heiles, 1984; Tenorio-Tagle & Bodenheimer, 1988). Heiles (1984), Brinks & Bajaja (1986), Puche et al. (1992), Mashchenko et al. (1999), Ehlerová & Palouš (2005) detected in the Milky Way, M31 and in the dwarf irregular galaxy Holmberg II (HoII) hundreds of neutral hydrogen shells whose radii range from a few tens to a thousand parsecs. On the other hand, Fabry-Perot observations of the ionized gas kinematics in many galaxies revealed a number of shells whose radii reach a few hundred parsecs and whose velocity pattern suggests an expansion with velocities up to 60 – 70 km s^{-1} (see, for example, Lozinskaya 1992; Chu et al. 1990; Oey & Massey, 1995; Valdez-Gutiérrez et al. 2001; Nazé et al. 2001; Lozinskaya et al. 2003; Relaño & Beckman, 2005 and references therein). The majority of these shells is associated with interior stellar clusters. The standard model (McCray & Kafatos, 1987; Mac Low & McCray 1988) was constructed with the energy injection from multiple supernovae explosions and stellar winds occurring in young stellar clusters which are often found inside small and intermediate sized shells. In such a case the energy supplied by supernovae and individual stellar winds is thermalized inside the parental stellar cluster, resulting in a high central overpressure which drives a high velocity outflow (the star cluster wind). This outflow, when interacting with the ambient interstellar medium (ISM), forms a leading and a reverse shocks which are separated by a contact discontinuity (see Figure 1). The interstellar gas collected by the outer shock forms an expanding shell which moves because the thermal pressure in the region C, between the reverse shock and the contact discontinuity, exceeds the ISM pressure. The swept-up gas cools rapidly and forms an expanding shell photoionized by the Lyman continuum from the embedded cluster. The number of ionizing photons rapidly drops with the star cluster age (Leitherer et al. 1999) and eventually (after ~ 10 Myrs) the driving cluster (or clusters) will find itself embedded inside a slowly expanding neutral hydrogen shell. The shell radius and velocity depend on the amount of energy released by the cluster and on the parameters of the ambient interstellar medium (see review by Bisnovatyi-Kogan & Silich, 1995 and references therein).

While the standard model is broadly consistent with the parameters of many small and intermediate sized structures found around young stellar clusters and OB associations (see, for example, the discussion of the superbubble growth discrepancy in Oey & García-Segura, 2004 and the analysis of the XMM-Newton observations of the 30 Dor C in Smith & Wang 2004), it meets a profound energy problem when applied to larger structures whose radii are comparable to the characteristic Z-scale of the density distribution in the host galaxy. For instance, Rhode et al. (1999) found that, in the case of the HoII galaxy, the stellar clusters found inside HI holes are unable to remove gas from these regions. Kim et al.

(1999) found only a weak correlation between the Large Magellanic Cloud (LMC) neutral hydrogen holes and the HII regions and concluded that the hypothesis of multiple supernovae is inconsistent with their data. Hatzidimitriou et al. (2005) cross-correlated the positions of 509 young neutral hydrogen shells detected in the Small Magellanic Cloud (SMC) with the locations of known OB-associations, Wolf-Rayet stars, supernova remnants and stellar clusters. They found that 59 shells have no young stellar objects associated with them despite the distributions of their radii and expansion velocities are consistent with those predicted by the multiple SNe model. They concluded that turbulence may be a promising mechanism that would allow us to understand the origin of these objects, but a quantitative comparison of the existing theory with observations is not possible at this moment.

Crosthwaite et al. (2000) examined the distribution of HI in the nearly face-on Scd galaxy IC 342 and did not find either the kinematic signatures specific to the expanding shells, or indications on the distortion of the observed structures by the differential galactic rotation, which is expected to be noticeable if the observed structures expand because of the energy output provided by the embedded stellar population (Palous et al. 1990; Silich, 1992). Therefore Crosthwaite et al. (2000) have concluded that the observed flocculent structure is formed via gravitational instabilities in a turbulent galactic disk, as suggested by Wada & Norman (1999), and not because of the energy output provided by the stellar component of the galaxy. Silich et al. (2006) have compared parameters of a ~ 500 pc radius HI ring detected in dwarf irregular galaxy IC 1613 with a combined energy output provided by a number of OB associations found inside the structure. They did not find a noticeable expansion velocity and concluded that the observed radius and mass of the structure are inconsistent with the SNe hypothesis.

Several other mechanisms that allow to shape the ISM of the host galaxy into large shell-like structures similar to those observed in nearby spiral and irregular galaxies, and that do not require violent stellar activity, include collisions of high velocity clouds with galactic disks (Tenorio-Tagle, 1981; Comeron & Torra, 1992), non-linear instabilities in the self-gravitating turbulent galactic disks (Wada et al. 2000; Dib & Burkert, 2004) and more exotic mechanisms such as the distortion of the ISM by powerful gamma-ray bursts (Efremov et al. 1999).

On the other hand, several modifications of the multiple SNe hypothesis have been suggested by different authors, in an attempt to reconcile the observed parameters of large HI structures with those predicted by the multiple supernovae model. Elmegreen & Chiang (1982) added the effects of the radiation pressure from field stars, that is able to provide additional expansion. Palous et al. (1990) added the effects of galactic rotation that distorts and stretches the shell along the direction of rotation. McClure-Griffiths et al. (2002) found

that some HI shells are located between the spiral arms of the Galaxy. They suggested then that density gradients that occur between the spiral arms and the interarm medium could result in the enhancement of the predicted sizes and migration of large shells from spiral arms into the interarm medium.

More recently, Relaño et al. (2007) have suggested that the population of ionized H_α shells associated with large HII regions (Rozas et al. 1996; Relaño & Beckman, 2005) may represent the precursors of the larger HI structures, and claimed that a very simplified analytic model is enough to explain larger HI objects. They assumed that young shells observed in H_α emission evolve in an energy dominated regime until the beginning of the supernova explosion phase, then make a transition to a momentum dominated stage and continue to expand with the momentum supplied by the embedded cluster during the initial time. The idea is not new (Dyson, 1980; Bruhweiler et al. 1980) and was used by Gil de Paz et al. (2002) and Silich et al. (2002), who discussed the origin of a giant ($R \approx 700$ pc) ring in the low-metallicity BCD galaxy Mrk 86. However, the key problem with this idea is that the momentum dominated regime is inefficient in driving bubble expansion because the thermal pressure in zone C (Figure 1) is approximately equal to the ram pressure of the ejected gas at the location of the reverse shock. Given that ram pressure drops as r^{-2}, the driving pressure equals the external pressure at a certain radius and the expansion quickly stalls after that point. Therefore we wonder how the early transition to the momentum dominated stage can solve the "energy crisis" that has been discussed by many authors during the last decades.

Here we re-analyze the hydrodynamical model presented in Relaño et al. (2007) keeping their assumption of a fast transition to the momentum dominated stage. We show that the over-simplified hydrodynamic equations and the "statistical" initial conditions adopted by them, which are not consistent with parameters for the largest HI structures, lead to overestimated expansion velocities and radii of the shells. Our results do not support their contention that H_α shells associated with the HII regions can be progenitors of the largest HI structures in the absence of any additional driving mechanism (for instance, radiation pressure from field stars, as suggested by Elmegreen & Chiang 1982).

The paper is organized as follows: in Section 2 we establish the main equations of our hydrodynamical model, and compare them with those used by Relaño et al. (2007). In Section 3 we first determine the initial conditions required to perform the numerical integration of the equations, and then present the resulting evolutionary tracks, our main result that small shells found in giant HII regions cannot be the progenitors of the largest neutral hydrogen supershells detected in gaseous galaxies.

2. Main equations

The kinetic energy supplied by supernovae and stellar winds from stellar clusters is thermalized by a shock, and this results in the four-zone structure discussed in Figure 1 (Castor et al. 1975; Weaver et al. 1977; Mac Low & McCray 1988; Bisnovatyi-Kogan & Silich 1995 and references therein). If thermal pressure in zone C suddenly drops, the radius of the reverse shock approaches the contact discontinuity, and the expansion of the outer shell is then supported directly by the momentum deposited by the stellar cluster (see, for example, Koo & McKee, 1992). Relaño et al. (2007) suggested that interstellar shells expanding around star forming regions reach this stage after a short while and then evolve in the momentum-dominated mode. We follow their assumption in the next sections, but note that it is in bad agreement with estimates of the characteristic cooling time in zone C (e.g., Figure 1 presented in Mac Low & McCray 1988). In the 2D or 3D cases, this regime occurs at the waist of the shell if a driving cluster is embedded into the disk-like density distribution (Gil de Paz et al., 2002; Silich et al., 2006). The expansion of the shell (or of some segments of the shell) is then defined by mass and momentum conservation:

$$M = M_0 + \frac{4\pi}{3}(R^3 - R_0^3)\rho_{ISM} + \dot{M}_{SC}(t - t_0), \tag{1}$$

$$\frac{\mathrm{d}}{\mathrm{d}t}(Mu) = -4\pi R^2(P_{ISM} - \rho_w V_\infty^2), \tag{2}$$

where M, u and R are the mass, expansion velocity and radius of the shell, respectively. R_0 is the initial radius of the shell, t_0 is the initial time and M_0 is the initial mass of the shell. The second term is the mass of the interstellar gas swept up by the expanding shell, and the last term in equation (1) is the amount of ejected matter that sticks to the shell from the inside. The right-hand part of equation (2) represents the difference between the ambient gas pressure, P_{ISM}, and the driving ram pressure of the ejecta. $\dot{M}_{SC}$ is the mass deposition rate provided by SNe explosions and stellar winds, $\rho_w(R)$ is the density of the ejected matter when it reaches the shell, and V_∞ is the terminal speed of the ejected matter.

We assume that the parameters of the cluster remain constant during the evolution, and that the expansion velocity of the shell is much smaller than that of the ejected matter, $u \ll V_\infty$. The mass deposition rate, $\dot{M}_{SC}$, and the density of the ejecta, $\rho_w(R)$, then are:

$$\dot{M}_{SC} = 2L_{SC}/V_\infty^2 \tag{3}$$

$$\rho_w = \dot{M}_{SC}/4\pi R^2 V_\infty, \tag{4}$$

where L_{SC} is the rate of mechanical energy supplied by supernovae and stellar winds.

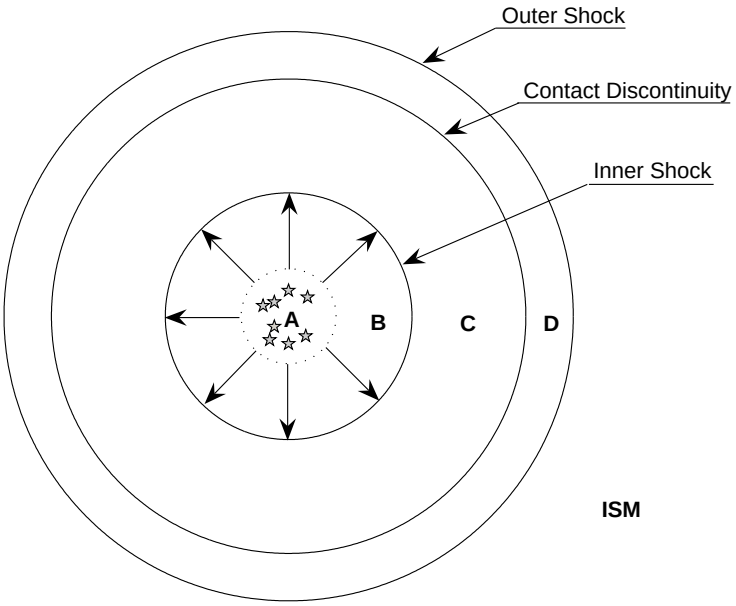

Fig. 1.— Schematic representation of the structure formed in the ISM by multiple stellar winds and supernovae explosions. The central zone (A) represents the stellar cluster where stellar winds and supernovae release their energy. The remaining concentric zones are the free-wind region (zone B), the shocked wind region (zone C), the shell of swept up interstellar matter (zone D) and the ambient ISM. When the shocked wind cools rapidly, zone C vanishes and the outer shell is pushed away by the momentum of the ejected matter.

Combining equations (1) and (2) one obtains:

$$\frac{\mathrm{d}u}{\mathrm{d}t} = -\frac{4\pi R^2 V_\infty^2 (P_{ISM} + \rho_{ISM} u^2) - 2L_{SC}(V_\infty - u)}{[M_0 + 4\pi\rho_{ISM}(R^3 - R_0^3)/3]V_\infty^2 + 2L_{SC}(t - t_0)} \tag{5}$$

$$\frac{\mathrm{d}R}{\mathrm{d}t} = u \tag{6}$$

One can solve these equations numerically for known values of R_0, M_0, u_0, ρ_{ISM}, L_{SC} and V_∞.

For the particular case when supernovae and stellar winds deposit all momentum instantaneously and the pressure in the interstellar medium is zero, $P_{ISM} = 0$, equations (1) and (2) become:

$$M(R) = M_0 + \frac{4\pi}{3}\rho_{ISM}(R^3 - R_0^3), \tag{7}$$

$$M(R)u(t) = M_0 u_0. \tag{8}$$

Furthermore, neglecting the mass of the star forming cloud and assuming

$$M_0 = \frac{4\pi}{3}\rho_{ISM} R_0^3, \tag{9}$$

the solutions are reduced to the set of the main equations (equations 1 and 2) used by Relaño et al. (2007):

$$R(t) = R_0 \left[1 + \frac{4u_0(t - t_0)}{R_0}\right]^{1/4}, \tag{10}$$

$$u(t) = \frac{3M_0 u_0}{4\pi\rho_{ISM} R^3}. \tag{11}$$

Thus, their main equations represent an oversimplified 1D model that neglects the effects of the ambient pressure, the mass of the star forming cloud and the continuous mechanical energy injection.

To illustrate the differences in the solutions of equations 5 and 6 and equations 10 and 11, we assume an interstellar gas density

$$\rho_{ISM} = \frac{3M_{HI}}{4\pi R_{HI}^3}, \tag{12}$$

where M_{HI} and R_{HI} are the mass and radius of an evolved HI shell (for the comparison we use the particular case of GSH 285-02+86, whose radius and mass are $R_{HI} = 385$ pc

and $M_{HI} = 44 \times 10^5$ $M_\odot$, respectively). The number density of the interstellar gas then is $n_{ISM} = 0.75$ cm^{-3}. We further assume that the initial radius of the shell is $R_0 = 104$ pc and obtain the initial mass of the shell, M_0, from equation (9). Then we use the observed velocity of the progenitor shell (64.7 km s^{-1}) as the initial value for the solution of equations 5 and 6. For the oversimplified case of equations 10 and 11 we use energy conservation, and the initial velocity in this case is

$$u_0 = \frac{2E_{kin}}{M_0}, \tag{13}$$

where the kinetic energy of the progenitor shell, $E_{kin} = 36.1 \times 10^{52}$ erg s^{-1}, has been derived from the Starburst99 synthetic model (Leitherer et al. 1999). Note that one cannot use identical initial conditions (the same initial velocity) in both approaches because in one case the energy and momentum are deposited instantaneously and, in the other, they are supplied continuously and grow with time during the shell evolution.

Figure 2 presents the expansion velocities predicted by both sets of equations. Certainly, the initial velocity in the oversimplified model is much larger than that of equations 5 and 6, but it drops faster. When the radius of the shell becomes about three or four times that of the initial value, the difference between the two calculations becomes small. Later on, the effect of the ambient pressure becomes important, but the shell continues to expand in the oversimplified model.

In the next section we drop all simplifications associated with the analytic solutions and solve equations (5) and (6) numerically.

3. The expansion of the momentum-dominated shell into the homogeneous ISM

3.1. Initial conditions

We start the integrations at the initial time, $t_0 = 10^6$ yr, and with the initial mass, M_0. We adopt initial radii, R_0, and expansion velocities, u_0, derived from the H$_\alpha$ observations of the ionized shells. R_0 is approximately 0.3 times the radius of the HII region, and u_0 is the observed velocity of the H$_\alpha$ shell. For example, in the case of NGC 1530-8, $R_0 = 104$ pc and $u_0 = 64.7$ km s^{-1}, respectively. In order to calculate the initial mass of the shell, we substitute into equation (9) the value of the initial radius and the average density 0.1 cm^{-3} assumed by Relaño et al. We also assume that the embedded cluster continuously expels the gas released by SNe and stellar winds, whose momentum supports the expansion of the outer shell, during ~ 40 Myr, the characteristic life-time of a $8\,M_\odot$ star - the lowest mass

star which will eventually explode as a supernova. Also, the pressure in the surrounding medium is explicitly included here.

We calculate the density of the ISM using the masses and radii of the HI shells and their progenitors:

$$\rho_{ISM} = \frac{M_{HI} - M_0}{\frac{4\pi}{3}(R_{HI}^3 - R_0^3)} \tag{14}$$

Thus, we derive the density of the ISM for each couple of HI and HII shells from their observed parameters. For instance, in the case of GSH 285-02+86, GSH 304–00-12 and GSH 305+01-24 from the list of McClure-Griffiths et al. (2002), the interstellar gas number density would be 0.75, 1.38 and 0.62 cm^{-3}, respectively, if one uses as the progenitor the HII shell N8 found by Relaño et al. (2007) in the spiral galaxy NGC 1530.

The average mechanical luminosity of the embedded cluster has been calculated from the Starburst99 synthetic model with an instantaneous burst of star formation (Leitherer et al. 1999). The average mechanical luminosity of the cluster then is:

$$L_{SC} = E_{SW+SN}/\tau, \tag{15}$$

where we use $\tau = 10$ Myr. The mechanical luminosities of the embedded clusters, as well as the initial masses, radii and velocities for all shells are listed in Table 1.

The temperature of the interstellar medium is assumed to be $T_{ISM} = 6000$K, which is a typical value in the warm neutral component of the ISM (Brinks, 1990). The thermal pressure in the ambient medium then is $P_{ISM} = k\ n_{ISM}\ T_{ISM}$, where k is the Boltzmann's constant and $n_{ISM} = \rho_{ISM}/m_H$ is the interstellar gas number density obtained from equation (14).

The last input parameter for our model, the terminal speed of the star cluster wind V_∞, is determined by the energy and mass deposition rates, and is close to the terminal velocity of individual stellar winds (Raga et al. 2001, Stevens & Hartwell 2003). We assume for our calculations that the star cluster wind terminal speed is constant and falls in the range $1500 - 3000$ km s^{-1} (e.g., Leitherer at al. 1999). Note that this parameter defines the amount of momentum deposited by the cluster and therefore affects the dynamics of the momentum-dominated shell.

3.2. Results and discussion

We calculate the evolutionary tracks for the HII shells associated with the list of large HII regions studied by Relaño et al. (2007), and compare them with the observed parameters

of the HI shells. For the comparison we have chosen three HI shells from the list of McClure-Griffiths et al. (2002) whose morphologies are close to the spherical shape: GSH 285-02+86, GSH 304-00-12 and GSH 305+01-24. They are representative of high, intermediate and low mass objects, respectively.

The results of the calculations are presented in Figure 3 and in Table 2. The top left panel in Figure 2 compares the results of the calculations with the parameters of low mass neutral shells. It shows that most of the HII shells detected in the giant HII regions certainly can evolve into objects whose parameters are identical to those of low mass HI shells. For example, in the case of GSH 305+01-24, nine out of the twelve HII shells (see Table 2) can easily reach the observed size of the HI shell having a proper mass (3.9×10^5 $M_\odot$) and an expansion velocity which is similar or even higher than the observed velocity of GSH 305+01-24. This implies that the HII shells found by Relaño et al. (2007) in giant HII regions can be progenitors of such low mass HI shells.

The top right panel in Figure 3 compares the evolutionary tracks of the progenitor shells with the observed parameters of the intermediate mass (1.9×10^6 $M_\odot$) HI object GSC 304-00-12. In this case only the four most energetic HII shells (NGC 1530-8, NGC 1530-22, NGC 3359-6 and NGC 6951-2) can eventually reach the required radius sweeping enough interstellar mass (see Table 2). However only two of them (NGC 1530-8 and NGC 6951-2) present the expansion velocities that are similar to the observed one. The expansion velocities of the rest fall well below the observed value. Thus GSC 304-00-12 represents a limit case that separates the low mass HI objects driven by multiple SNe explosions from the largest ones whose parameters are not consistent with the multiple SNe hypothesis. The latter case is illustrated by the bottom panel in Figure 3.

The bottom panel compares the evolutionary tracks of Relaño's shells with parameters of the very massive shell GSH 285-02+86, whose mass is 4.4×10^6 $M_\odot$ (McClure-Griffiths et al. 2002). Here we also present (dashed line) the expansion velocity predicted by the analytic model for NGC 1530-8, the most energetic shell from the list of Relaño et al. (2005). The plot clearly demonstrates that the analytic model leads to overestimated expansion velocities. This is because the analytic calculations adopt a low value for the interstellar gas density which is not consistent with the masses and radii of the most massive neutral shells (in the analytic approach the mass of the shell is only 0.6×10^6 $M_\odot$ when its radius reaches the observed value of 385 pc, whereas in our calculations it is 4.4×10^6 $M_\odot$).

The bottom panel in Figure 3 shows that HII shells found by Relaño et al. (2005) inside giant HII regions can never evolve into the largest and most massive neutral hydrogen supershells. In this case the energy and momentum supplied by the central cluster are not sufficient to make the evolution from the original shell finally fit all the observed parameters

of the HI supershell: its mass, radius and expansion velocity. In this case only the three most energetic progenitor shells (NGC 1530-8, NGC 3359-6 and NGC 6951-2) can reach a size and accumulate a mass that are comparable to those of GSH 285-02+86. However, in all these cases the model predicted expansion velocities are much smaller than that measured by McClure-Griffiths et al. (2002) for GSH 285-02+86. This implies that, contrary to the statement made by Relaño et al. (2007), the young ionized shells found in giant HII regions cannot evolve into the largest HI supershells (i.e., eventually fit simultaneously the mass, radius and expansion velocity of the HI object) unless some additional physical mechanism, other than the multiple supernovae explosions, contributes to the formation of the largest shells at the later stages of their evolution.

Figure 3 presents the results of the calculations under the assumption that the star cluster terminal speed is $V_\infty = 1500$ km s^{-1}. In order to learn how this parameter affects our results we have provided a set of numerical calculations with initial conditions which are identical to those used in the case of GSH 285-02+86 (Figure 3, bottom panel) but with a star cluster wind terminal speed twice as large as the previous one: $V_\infty = 3000$ km s^{-1}. The results of these calculations are presented in Figure 4 which demonstrates that the model predicted expansion velocity becomes smaller when the star cluster wind terminal speed grows up. This implies that one cannot avoid the discrepancy between the predicted and the observed velocities by varying the star cluster wind terminal speed within a reasonable velocity interval.

4. Conclusions

Here we have critically examined the evolution of the ionized shells found inside giant HII regions, as predicted by the multiple SNe model in one dimension. We have used the observed parameters of the HII shells as initial conditions for our numerical model and compared the results of the calculations with three representative cases of low, intermediate and high mass HI objects from the list of McClure-Griffiths et al. (2002).

We have found that the ionized shells observed within giant HII regions cannot evolve into the largest neutral hydrogen supershells if the multiple supernovae explosions of massive stars is the only driving mechanism. Some additional physical mechanism must contribute to the formation of the largest shells for the model to be in agreement with the observed parameters of the most massive neutral hydrogen supershells detected in our and other galaxies.

Note that spherically-symmetric models must be taken with care when compared with

objects whose radii are comparable with several characteristic scale heights in the ISM density distribution. If that is the case, the expansion velocities at the top and at the waist of the shell are different and the shell acquires a distorted hour-glass form. The majority of the swept-up interstellar matter is concentrated in a thin layer nearby the plane of the host galaxy. 3D calculations are then required in order to investigate the shell's morphology and kinematics in the differentially rotating galactic disk (see, for example, Silich et al. 1996).

We thank an anonymous referee for central comments and suggestions which helped us to clarify our formulations and improve the quality of the paper. We also appreciate usuful comments from our Korean and Mexican colleagues during the IV Korea-Mexico workshop in Daejon. This study has been supported by Conacyt (México) grant 47534-F.

REFERENCES

Bisnovatyi-Kogan, G. S. & Silich, S. A. 1995, Rev. Mod. Phys. 67, 661

Brinks, E., 1990, ASSL, 161, 39

Brinks, E. & Bajaja, E. 1986, A&A, 169, 14

Bruhweiler, F.C., Gull, T.R., Kafatos, M. & Sofia, S. 1980, ApJL, 238, 27

Castor, J., McCray, R. & Weaver, R., 1975, ApJ, 200, 107

Chu, Y.-H. & Mac Low, M.-M. 1990, ApJ, 365, 510

Comeron, F. & Torra, J. 1992, A&A, 349, 41

Crosthwaite L.P., Turner, J.L. & Ho, P.T.P. 2000, AJ, 119, 1720

Dib, S. & Burkert, A. 2004, Ap&SS, 292, 135

Dyson, J.E. 1980, Physics of the Interstellar Medium, NY, John Wiley & Sons, 145

Efremov, Y. N., Ehlerová, S. & Palouš, J. 1999, ApJ, 350, 457

Ehlerová, S. & Palouš, J. 2005, A&A, 437, 101

Elmegreen, B. G. & Chiang, W.-H. 1982, ApJ, 253, 666

Gil de Paz, A., Silich, S.A., Madore, B.,F., Sánchez Contreras, C., Zamorano, J. & Gallego, J. 2002, ApJ, 573, 101

Hatzidimitriou, D., Stanimirovic, S., Maragoudaki, F., Stavely-Smith, L., Dapergolas, A. & Bratsolis, E. 2005, MNRAS, 360, 1171

Heiles, C. 1980, ApJ, 235, 833

Heiles, C. 1984, ApJS, 55, 585

Kim, S., Dopita, M. A., Stavelet-Smith, L. & Bessel, M. 1999, A&A, 350, 230

Koo, B.-C. & McKee, C.F., 1992, ApJ, 388, 93

Leitherer, C., et al. 1999, ApJS, 123, 3

Lozinskaya, T.A. 1992, Supernova and Stellar Wind in the Interstellar Medium, AIP, NY, 223p.

Lozinskaya, T., Moiseev, A., Podorvanyuk, N., 2003, Astronomy Letters, 29, 77, (astro-ph/0301214)

Mac Low, M.-M. & McCray, R. 1988, ApJ, 324, 776

Mashchenko, S.Y., Thilker, D.A. & Braun, R. 1999, A&A, 343, 352

McClure-Griffiths, N.M., Dickey, J.M., Gaensler, B.M. & Green, A.J. 2002, AJ, 578, 176

McCray, R. & Kafatos, M. 1987, ApJ, 317, 190

Nazé, Y., Chu, Y.-H., Points, S.D., Danforth, C.W.; Rosado, M. & Chen, C.-H.R.

Oey, M.S. & García-Segura, G., 2004, ApJ, 613, 302

Oey, M.S. & Massey, P. 1995, ApJ, 452, 210

Palous J., Franco, J. & Tenorio-Tagle, G. 1990, Astron. Astrophys. 227, 175

Puche, D., Westpfahl, D., Brinks, E. & Roy, J-R. 1992, AJ, 103, 1841

Raga, A.C., Velázquez, P.F., Cantó, J., Masciadri, E., Rodríguez, L.F., 2001, ApJ, 559, 33

Relaño, M. & Beckman, J.E. 2005 A&A, 430, 911

Relaño, M., Beckman, J.E., Daigle, O., Carignan, C. 2007, A&A, 467, 1117

Rhode, K. L., Salzer, J. J., Westpfahl, D. & Radice, L. A. 1999, AJ, 118, 323

Rozas, M., Beckman, J.E. & Knapen, J-H. 1996, A&A, 307, 735

Silich, S.A. 1992, Ap&SS 195, 317.

Silich, S.A., Franco, J., Palouš & Tenorio-Tagle, G. 1996, ApJ, 468, 722

Silich, S.A., Tenorio-Tagle G., Muñoz-Tuñon, C., Cairos L.-M. & Gil de Paz A., 2002, in ASP Conf. Ser. 282 "Galaxies: The Third Dimension" Edts. M. Rosado, L. Binette & L. Arias, p58

Silich, S., Lozinskaya, T., Moisseev, A., Podorvanuk, N., Rosado, M., Borissova, J. & Valdez-Gutiérrez, M. 2006, Astron. Astrophys., 448, 123

Smith, D.A. & Wang, Q.D., 2004, ApJ, 611, 881

Stevens, I.R. & Hartwell, J.M., 2003, MNRAS, 339, 280

Tenorio-Tagle, G. 1981, Astron. Astrophys. 94, 338

Tenorio-Tagle, G. & Bodenheimer, P., 1988, ARA&A, 26, 145

Valdez-Gutiérrez M., Rosado M., Georgiev L., Borissova J., Kurtev R. 2001, Astron. Astrophys., 366, 35.

Wada, K. & Norman, C.A. 1999, ApJ, 516, L13

Wada, K., Spaans, M. & Kim, S., 2000, ApJ, 540, 797

Weaver, R., McCray, R., Castor, J., Shapiro, P., Moore, R., 1977, ApJ, 218, 377

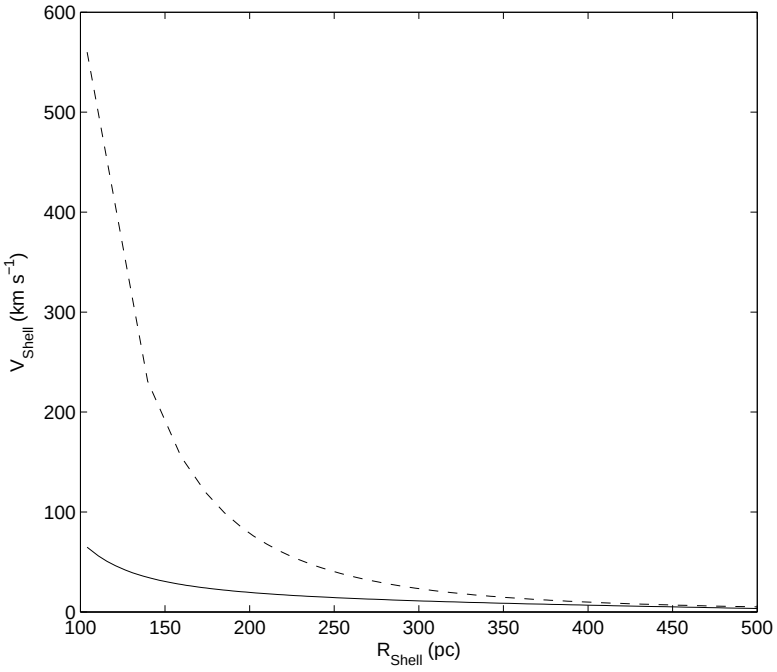

Fig. 2.— The comparison of analytic results with numerical models (the example corresponds to the HI shell GSH 285-02+86 and the HII progenitor shell NGC 1530-8). The solid line represents the numeric solution of equations 5 and 6. The dashed line is the analytic solution of equations 10 and 11. The initial radii and masses of the shells are identical in both calculations, however the initial velocities are different. This is because the analytic formulation is based on the assumption that all energy and momentum are deposited instantaneously at the beginning of the momentum dominated stage, whereas the numerical model assumes that the energy and momentum are supplied continuously until the last supernova explosion.

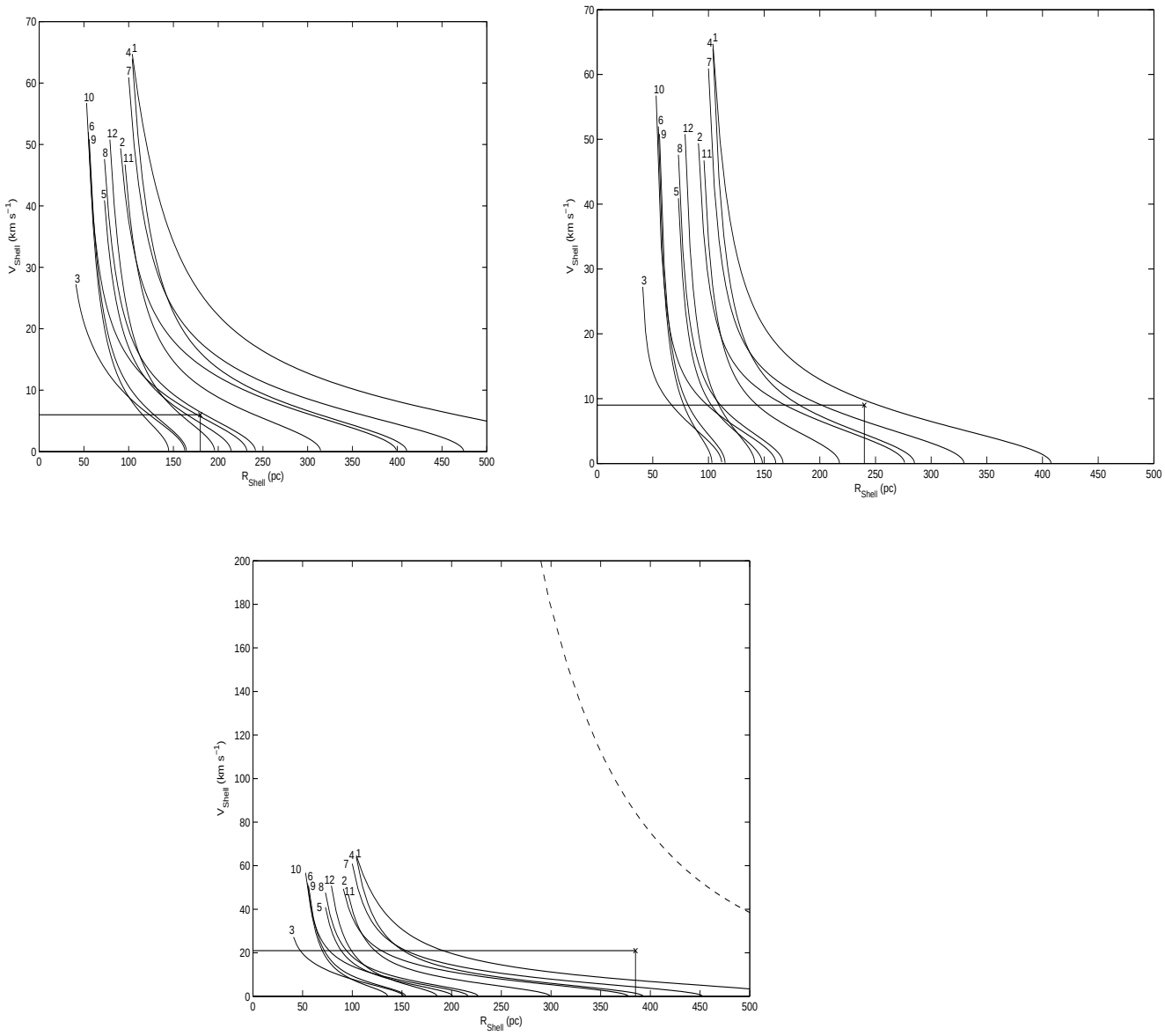

Fig. 3.— The comparison of the predicted expansion velocities with the observed values. The results of the calculations are compared with parameters of low, intermediate and high mass objects from the list of McClure-Griffiths et al. (2002). Different lines correspond to different initial conditions (associated with 12 HII progenitor shells from the list of Relaño et al. 2007). The lines are labeled with the numbers that identify the progenitor shells in Table 1. The observed velocities and radii of the HI shells are marked by the horizontal and vertical lines, respectively. The top left panel compares the model predicted radii and velocities with that of the HI supershell GSH 305+01-24 from the list of McClure-Griffiths et al. (2002). Similarly, the top right and bottom panels present the results for the more massive supershells GSH 304-00-12 and GSH 285-02+86 (the dashed line in the latter is Relaño's et al. analytic solution for NGC 1530-8). A 1500 km s^{-1} star cluster wind terminal speed was adopted for all calculations.

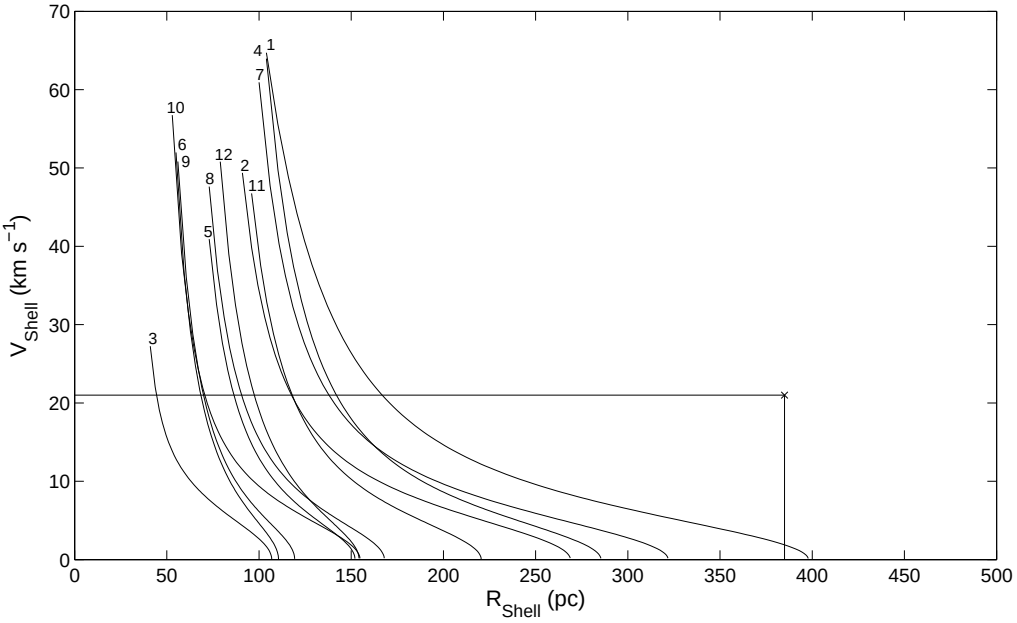

Fig. 4.— The impact of the star cluster wind terminal speed on the shell evolution. The calculations were performed for the HI shell GSH 285-02+86, with a star cluster wind terminal speed $V_\infty = 3000$ km s^{-1}. This can be compared with that presented in Figure 3 (bottom panel) where a value of $V_\infty = 1500$ km s^{-1} for the wind terminal speed has been adopted.

Table 1. Initial conditions

ID	Name	M_0 $10^4 M_\odot$	R_0 pc	u_0 $km\ s^{-1}$	L $10^{38} erg\ s^{-1}$
1	NGC 1530–8	8.9	104	64.72	11.4
2	NGC 1530–22	3.7	91	49.38	5.3
3	NGC 1530–92	0.3	41	27.24	0.9
4	NGC 3359–6	5.5	104	63.97	5.7
5	NGC 3359–42	1.9	73	40.91	1.5
6	NGC 3359–92	0.8	55	51.98	0.6
7	NGC 6951–2	4.8	100	60.93	7.6
8	NGC 6951–18	1.9	73	47.62	1.9
9	NGC 6951–41	0.8	56	50.82	0.9
10	NGC 5194–312	0.7	53	56.75	1.7
11	NGC 5194–403	4.2	96	46.75	3.3
12	NGC 5194–416	2.3	79	50.80	1.2

Table 2: Model predictions

		GSH 285–02+86			GSH 304–00-12			GSH 305+01-24		
ID	Name	M $10^5 M_\odot$	R pc	V kms^{-1}	M $10^5 M_\odot$	R pc	V kms^{-1}	M $10^5 M_\odot$	R pc	V kms^{-1}
Observed parameters										
		44	$375 - 395$	21	19	$200 - 280$	9	3.9	$140 - 220$	6
Predicted parameters										
1	NGC 1530–8	44	385	7.4	19	240	9.7	3.9	179	26.1
2	NGC 1530–22	42	378	0.1	19	240	3.9	3.9	179	14.2
3	NGC 1530–92	27	152	0.0	19	112	0.2	2.9	163	0.2
4	NGC 3359–6	44	385	1.4	19	240	4.5	3.9	180	16.1
5	NGC 3359–42	6.2	201	0.1	4.3	148	0.0	3.9	180	4.6
6	NGC 3359–92	1.9	136	0.0	14	103	0.1	2.0	145	0.1
7	NGC 6951–2	44	385	4.3	19	240	6.5	3.9	180	17.8
8	NGC 6951–18	9.0	227	0.0	6.2	167	0.1	3.9	180	6.5
9	NGC 6951–41	2.8	154	0.0	1.9	115	0.1	3.0	165	0.2
10	NGC 5194–312	7.9	217	0.1	5.6	160	0.1	3.9	180	5.7
11	NGC 5194–403	21	299	0.1	14	218	0.0	3.9	180	10.7
12	NGC 5194–416	4.8	185	0.1	3.5	142	0.0	3.9	180	3.4